*Physical Modelling in Geotechnics*


# Field and centrifuge modelling of a pumped underground hydroelectric energy storage system in sand

A. Franza & K.K. Sorensen
*Department of Civil and Architectural Engineering, Aarhus University, Aarhus, Denmark*

H.H. Stutz
*Institute of Soil Mechanics and Rock Mechanics, Karlsruhe Institute of Technology, Karlsruhe, Germany*

A. Pettey, C. Heron & A. Marshall
*Department of Civil Engineering, University of Nottingham, Nottingham, UK*

**ABSTRACT:** This paper presents a physical test campaign, including both a field trial and a centrifuge test series, to characterise the geotechnical performance of Underground Pumped Hydroelectric Energy Storage (UPHS) systems in sand. This system consists of a water filled geomembrane-lined reservoir that is pressurised by overburden sand and inflated/deflated to store/recover energy. To achieve a greater storage density per unit area, a geometry involving a "reverse configuration" of the geomembrane is adopted. The paper presents the geometry of the models, ground and membrane properties, while discussing simplifying experimental assumptions. Results illustrate the cyclic response of the UPHS system (focusing on overburden surface movements and pressure-volume relationship at the reservoir) to characterise its key mechanical performance and energy efficiency.

**Keywords:** field trial, centrifuge modelling, membrane, energy storage, reservoir.

## 1 INTRODUCTION

Underground Pumped Hydroelectric Energy Storage (UPHS) systems in sand, shown in Fig. 1, can be used to store excess energy from renewable (and traditional) sources (Olsen et al., 2015). Energy is stored by inflating a relatively flexible geomembrane–lined bag with water (referred to as underground "reservoir") that is pressurised by overburden soil; stored energy is recovered by deflating the reservoir and having the pressurised flow acting on a turbine. The input $E_i$ and output $E_o$ stored energy can be calculated by integrating the reservoir pressure $p$ with respect to the volume from the initial $V_i$ to the final volume $V_f$ and vice versa, respectively, giving an energy loss $\Delta E$ and an efficiency $\eta = E_o/E_i$ for a given cycle.

$$\Delta E = E_i - E_o = \int_{V_i}^{V_f} p \ dV - \int_{V_f}^{V_i} p \ dV \qquad (1)$$

The capacity $E_i$ and efficiency $\eta$ under inflation/deflation cycles can be affected by geometrical changes, irreversible (plastic) deformations of materials, and interface friction losses, along with losses in the piping and turbine/pump system. To prevent excessive tensile deformations of the membrane, an "initial reverse configuration" of the geomembrane–lined bag (see Fig. 1a) is considered.

This paper presents centrifuge and field testing of UPHS systems in sand. Preliminary results from cyclic experiments describe overburden surface movements, the relationship between reservoir pressure and volume, and observed energy system/storage performance.

## 2 FIELD TRIAL AT FOULUM

A 1:10 scale field trial of a full–size UPHS system shown in Fig. 1a was carried out at Aarhus University in Foulum, Denmark. At the site, boreholes reported 0.5 m of topsoil, 0 - 2.5 m sand till, below which is a uniform medium layer of meltwater sand. The water table is below the reservoir depth.

The setup consist of an underground reservoir and water basin with a trench in between for the automatic loop pumping system (pipes, pump, valves) to control and measure the in/out reservoir flow of water. Figs. 1b and c display the cross-section and an aerial view (prior to overburden earthworks). The underground reservoir has a side $L$ = 20 m, corner radius of 2 m, lift height $U_{lift}$ = 1.2 m, 1:2 slopes at the edges, soil cover $C$ = 2 m (testing with 4 m is envisioned). The inlet/outlet was situated centrally at the base of the bag.

To protect the geomembrane, a geotextile layer was placed around the bag. The overburden was constructed using excavated sand in 0.8 m thick compacted layers.

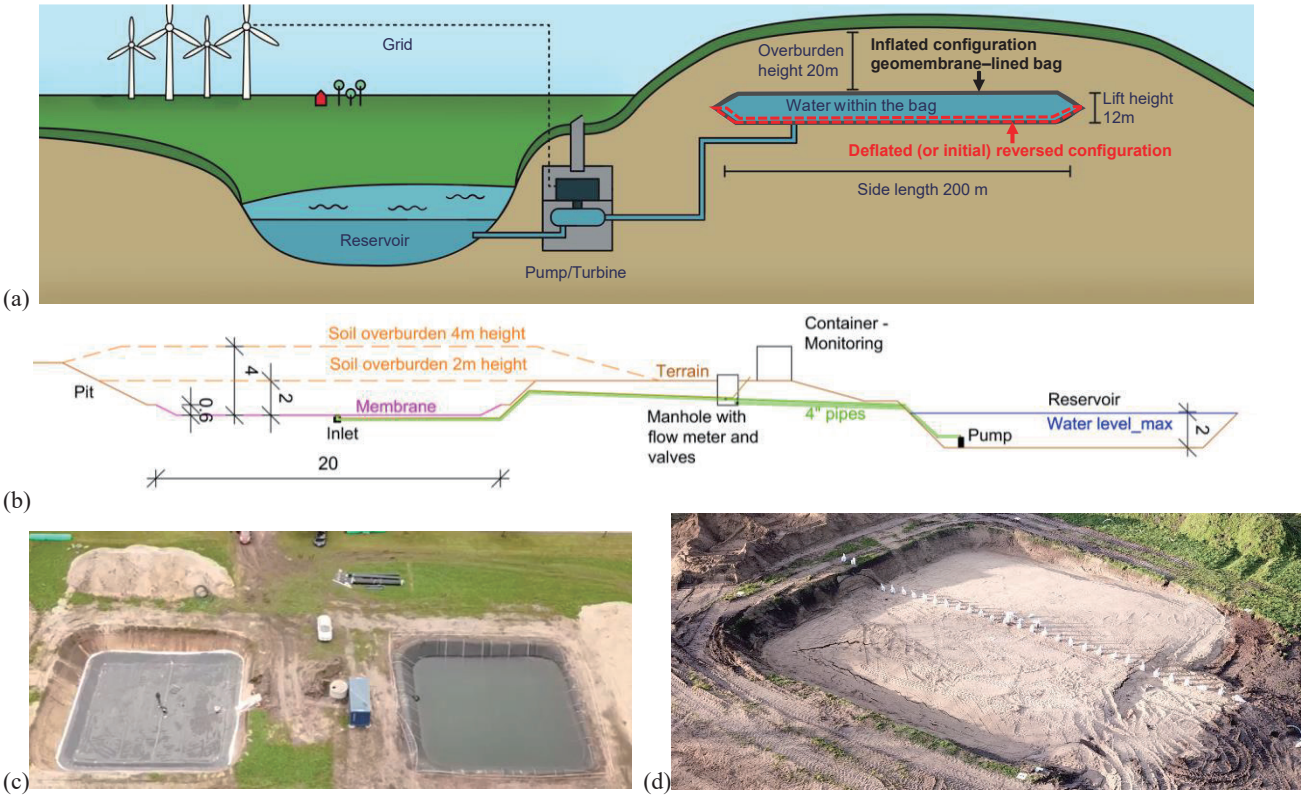


Fig. 1. (a) Functional principle of geomembrane–lined bag for UPHS at full scale prototype; (b) cross-section of the field trial at 1:10 scale; aerial views following (c) the geomembrane-lined bag installation and (d) the first cycle series and leakage test (4th Jan 2021).

Classification testing on representative samples of the overburden sand gave; specific gravity $G_s = 2.65$ g/cm³, $d_{50} = 0.30$ mm, and $d_{60} / d_{10} = 4.7$, $e_{min} = 0.369$, and $e_{max} = 0.699$. A relative density $I_D \approx 72\%$ of the overburden after compaction is estimated from a measured average in-situ dry density $\rho_d = 1813$ kg/m$^3$ and bulk density $\rho = 1973$ kg/m$^3$ using nuclear density method. The geomembrane is polypropylene-polyethylene GSE ProFlex (Solmax) having 2.0 mm thickness, density of 0.89 g/cm$^3$, elastic Young's modulus of 90 Mpa, elastic cyclic regime up to 5% biaxial strains and elongation at break of 19 %.

For brevity, only key measurements of pressure at the reservoir base ($P$) and water volume ($V$) are reported. These are respectively normalised by the initial vertical stress at the geomembrane prior to inflation ($P_0$) and the nominal volume ($V_0$) corresponding to a fully inflated reverse shape configuration with $U_{lift} = 1.2$ m (see Fig. 1b). For the field trial, $V_0 = 428.6$ m$^3$ and $P_0 = 37$ kPa, with the latter value being close to the vertical total stress estimated from bulk density and cover. In particular, pressures $P_A$ and $P_B$ were measured by piezometers located within the underground reservoir at its base next to the central inlet while $P_C$ is at one of the bag corners; the central pressure $P_A$ used by the pumping control system is logged at a frequency of 0.1 Hz whereas a stand-alone datalogger reads $P_B$ and $P_C$ at 0.016 Hz. Note that reservoir pressures $P$ due to water and soil stresses are estimated as $P = P^* +$ (101.325 kPa$-P_{atm}$), where temperature compensated pressure values measured by the piezometers ($P^*$) are corrected by the fluctuation in the barometric atmospheric pressure $P_{atm}$, remotely obtained from the local automatic climate station number 6069. The reservoir volume $V$ is obtained by the integration of the in/out water flow.

The first part of the field campaign is described. The first cycle series up to a maximum volume $V = 150$ m$^3$ associated with an inflation/deflation sequence as $R_v = V/V_0 = [0, 0.35, 0.05, 0.35, 0.06, 0.35]$ (over 22.5 days,), followed by a leakage test at a constant volume ratio $R_v = 0.35$ (lasted 17 days). Fig. 2a and b display reservoir pressure and volume (against time in days) from cycles 1 and 2-3, respectively; initial time $t = 0$ corresponding to 24th Nov 2021 14:23. Fig. 3c shows the relationship between reservoir normalised pressure and volume. The hysteretic area enclosed within a cycle is associated with the energy loss.

Central pressures $P_A$ and $P_B$ nearly match the corner pressure $P_C$ (when reduced by 0.9 kPa), confirming the reliability of the piezometers and logging systems. Furthermore, dynamic pressures are negligible close to the inlet, except for volumes V < 20 m$^3$ ($R_v < 0.05$): in Fig. 3, deflation volumes below 20 m$^3$ are associated with a transient steep decreasing rate of

pressure to $P_A/P_{A,0} = 0.27$ followed by a recovery to 0.97 when the flow ceases. To prevent large dynamic pressure and/or closing the inlet, a minimum volume threshold at which the flow is inverted is set to 25 m$^3$ ($R_v = 0.06$) starting from cycle 2. Finally, constant pressure values from the constant volume test (results are omitted) confirmed that creep and leakage was negligible, while Fig. 1d indicates a balloon-type inflation of the underground reservoir with concave shape of the overburden.

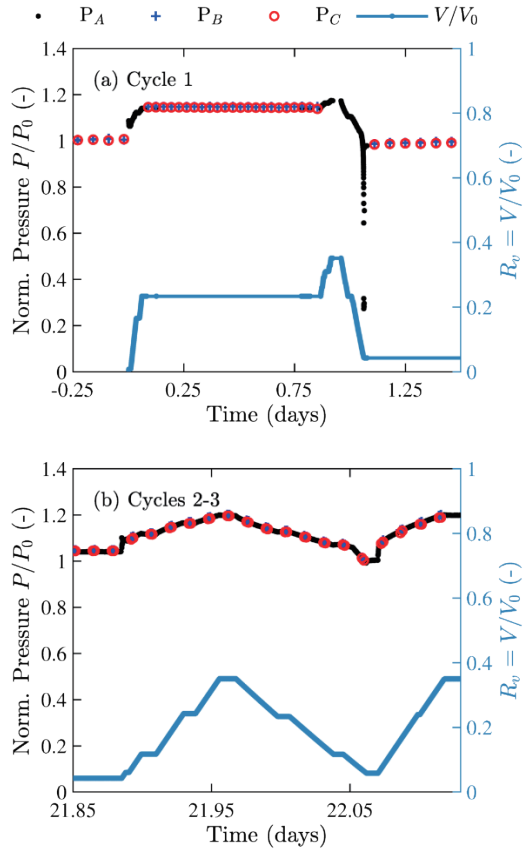


Fig. 2. Field pressure and volume ratio against time.

The pressure-volume response in Fig. 3 agrees qualitatively with the trends observed by Sørensen et al. (2021) for a smaller laboratory reduced scale UPHS experiment at 1g. The field system had a lower rate of pressure increase per inflated volume (i.e. inflation slope) during cycle 1 compared with subsequent cycles 2 and 3, whereas the deflation slope for all cycles is nearly identical and larger in magnitude than the inflation values. Also, when the flow is inverted, inflation curves of cycles 2 and 3 are characterised by a steep increase to $P_A/P_{A,0} > 1$. This is followed by a nearly linear increase up to reservoir bottom pressure $P_{A,max}/P_{A,0} = 1.2$, which is associated with an increase of the initial pressures $P_{A,max} - P_{A,0} = 7.4$ kPa. It is found that the pressure increase is significantly larger than the estimated increase in water pressure from hydrostatic conditions. Also, the deflation curve of cycle 2 has a distinct toe kick at a volume ratio of approximately $R_V = 0.1$. Importantly, $P - V$ curves indicate that arching and in-locked stresses within the soil above the reservoir may develop during the first cycle, leading to: maximum pressure values greater than the self-weight of the water and soil only during inflation; stresses lower than soil self-weight only during deflation. The efficiency $\eta$ estimated from the input and output energies of both cycles 1 and 2 is approximately 96 %, which is higher than the 85 % values reported for lower stress tests (Sørensen et al., 2021).

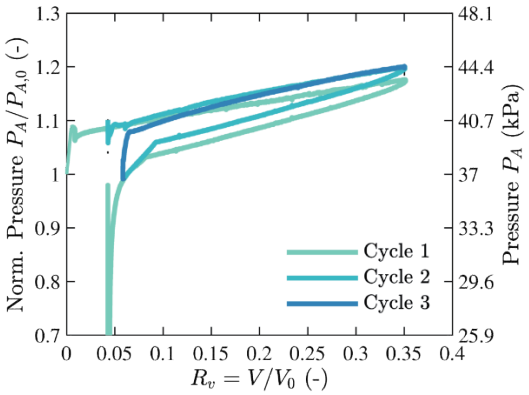


Fig. 3. Relationship between field pressure and volume.

## 3 CENTRIFUGE TESTING

A 1/80$^{th}$ scale (of field trial) experimental package was tested at a nominal elevated-gravity field of 80 g in the University of Nottingham geotechnical centrifuge. As in Fig. 4, the reservoir buried in sand is modelled as a single latex layer, filled with water, and fixed at the edges by a clamp system to an aluminium plate that models the bottom-fixed lining of the reservoir. The reservoir has side lengths $L = 250$ mm, a lift height $U_{lift} = 7.5$ mm, and cover $C = 25$ mm. Dry Congleton CNHST95 sand was air pluviated to achieve a loose relative density. The geomembrane is modelled as single latex layer, with a thickness of 0.5 mm to replicate the prototype stiffness of the field trial geomembrane lining. A volume-controlled system is used for inflight inflation/deflation of the water reservoir, consisting of a linear actuator, a piston, solenoid valves, an LVDT, and piping. A pore pressure transducer is used to measure the model-reservoir pressure $P$ while its volume $V$ can reach 1.5 $V_0$. Digital cameras are used to take images of the soil surface.

Following model preparation, the experimental set-up was mounted on the centrifuge, spun-up to 80 g, and then the reservoir volume was varied for three cycles having the sequence $R_v = [0, 1.5, 0.5, 1.0, 0.5, 1.0, 0.5]$. Cycle 1 up to 1.5 $V_0$ evaluates the stability, while cycles 2 and 3 up to 1.0 $V_0$ simulate service performance. The

initial reservoir pressure was $P_0 \approx 36$ kPa.

Figs. 5a and b display the overburden surface during the first inflation, characterised by balloon and terracing shapes for $R_v = 0.5$ and 1.25, respectively, having concave and convex profiles at the centre. The surface soil above the edges of the reservoir was pushed outwards during cycle 1, affecting subsequent cycles.

Fig. 5f plots the centrifuge $P$–$R_v$ relationship. As for the field trial, cycle 1 displays a nearly linear increase in pressure with volume up to $1.35\,P_0$ and a greater linear deflation rate that resulted in a minimum $P = 0.8\,P_0$. Interestingly, cycles 2 and 3 are nearly identical: inflation curves nearly linear, with $P > P_0$, and slopes similar to cycle 1; nonlinear deflation curves having a kick-toe shape and reaching the minimum pressure $0.8\,P_0$ experienced during deflation cycle 1. The efficiency of cycles 2 and 3 is 92.2%, which is lower than for the field trial due to the kick-toe shape.

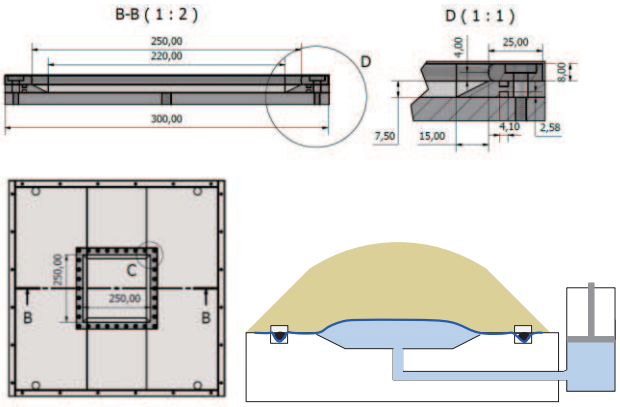


Fig. 4. Drawings of the base plate and clamp system (in mm) and conceptual design of the model.

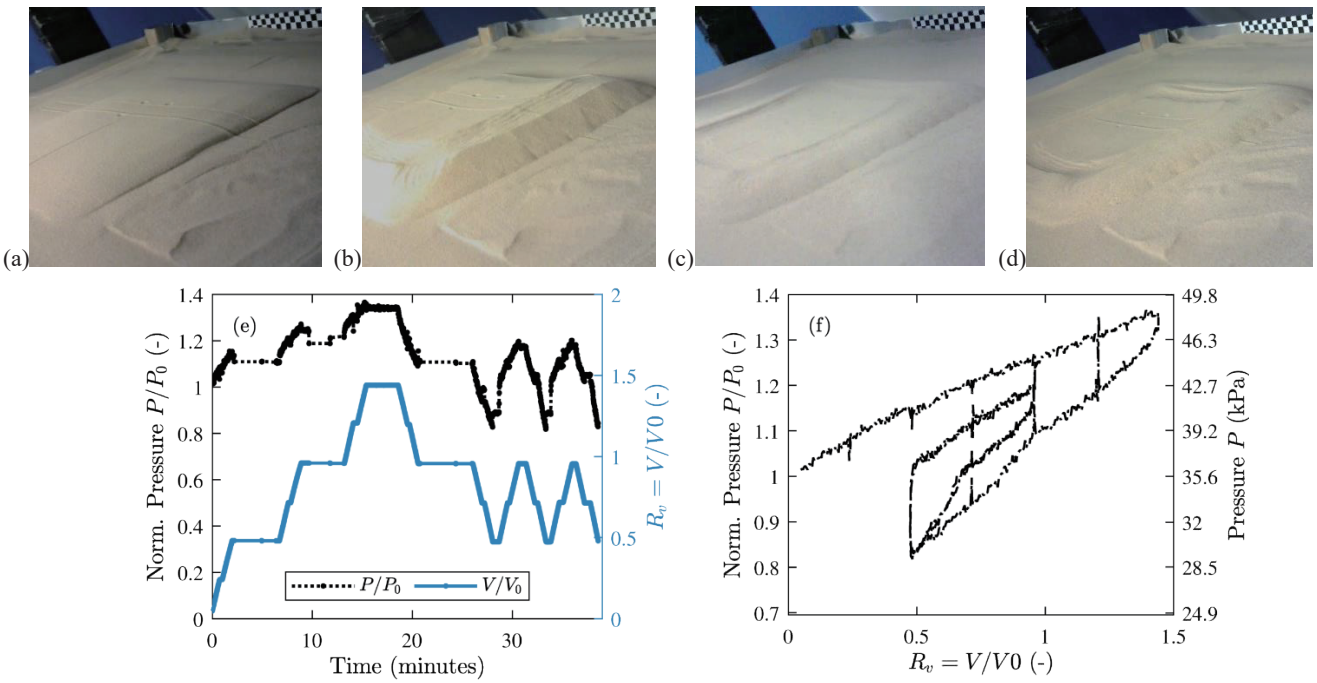


Fig. 5. Overburden displacements during the first cycle at (a)-(b)-(c) $R_v = 0.5$, 1.25, 0.5 and (d) the final state at $R_v = 0.5$. Centrifuge measurements showing (e) reservoir pressure with volume ratio plotted against time as well as (f) pressure-volume ratio relationship.

## 4 CONCLUSIONS

Preliminary results indicated that UPHS efficiency in sand from1g and elevated-gravity models at 1:10 scale are higher than values collected at lower stresses, with energy losses in the overburden and reservoir varying between 3% and 8% (and possibly increasing with the maximum inflation volume). Further testing is ongoing to characterise both the tested sands as well as the deformation mechanism and stability of the overburden.

## ACKNOWLEDGEMENTS

This research was supported by Energiteknologiske Udviklings- og Demonstrationsprogram (EUDP).

## REFERENCES

Olsen, J., Paasch, K., Lassen, B., & Veje, C. T. (2015). A new principle for underground pumped hydroelectric storage. J. Energy Storage, 2, 54–63.

Sørensen, K. K., Stutz, H. H., Brødsgaard-Raptis, P. & Luxhøj, M. 2021. Conceptual physical modelling of a subsurface geomembrane energy storage system. In *Proc. 20th Intern. Conf. Soil Mech. Geotech. Eng.*